ACS OMEGA

http://pubs.acs.org/journal/acsodf

Article

Network Analysis of the Herb−Drug Interactions of Citrus Herbs Inspired by the "Grapefruit Juice Effect"

Jintao Lü, Dan Zhang, Xiaomeng Zhang, Rina Sa, Xiaofang Wang, Huanzhang Wu, Zhijian Lin, and Bing Zhang*

Cite This: *ACS Omega* 2022, 7, 35911−35923

Read Online

ACCESS | Metrics & More | Article Recommendations | Supporting Information

ABSTRACT: This study was performed to investigate the herb−drug interactions (HDIs) of citrus herbs (CHs), which was inspired by the "grapefruit (GF) juice effect". Based on network analysis, a total of 249 components in GF and 159 compounds in CHs exhibited great potential as active ingredients. Moreover, 360 GF-related genes, 422 CH-related genes, and 111 genes associated with drug transport and metabolism were collected, while 25 and 26 overlapping genes were identified. In compound−target networks, the degrees of naringenin, isopimpinellin, apigenin, sinensetin, and isoimperatorin were higher, and the results of protein−protein interaction indicated the hub role of UGT1A1 and CYP3A4. Conventional drugs such as erlotinib, nilotinib, tamoxifen, theophylline, venlafaxine, and verapamil were associated with GF and CHs via multiple drug transporters and drug-metabolizing enzymes. Remarkably, GF and CHs shared 48 potential active compounds, among which naringenin, tangeretin, nobiletin, and apigenin possessed more interactions with targets. Drug metabolism by cytochrome P450 stood out in the mutual mechanism of GF and CHs. Molecular docking was utilized to elevate the protein−ligand binding potential of naringenin, tangeretin, nobiletin, and apigenin with UGT1A1 and CYP3A4. Furthermore, in vitro experiments demonstrated their regulating effect. Overall, this approach provided predictions on the HDIs of CHs, and they were tentatively verified through molecular docking and cell tests. Moreover, there is a demand for clinical and experimental evidence to support the prediction.

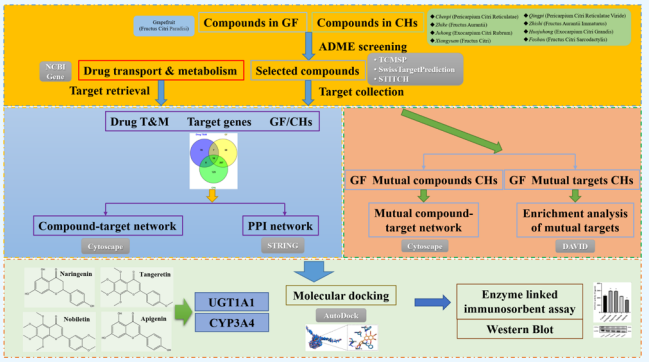

1. INTRODUCTION

As traditional herbal medicines are popularly applied, herb−drug interactions (HDIs) have become a rising concern in the clinical use of conventional drugs. Complicated chemical compositions and potential multiple bioactivities are associated with complex HDIs. Based on different interaction pathways, HDIs can be classified into pharmacokinetic interactions and pharmacodynamic interactions, and the former ones were the focus of past studies, which concentrated on drug transport and metabolism. HDIs may end up quite differently: on the one hand, they affect drug levels and/or activities and therefore potentially cause therapeutic failure or adverse reactions; on the other hand, some HDIs lead to beneficial clinical effects including heightened efficacy and lessened side effects.[1]

The consumption of grapefruit (GF), a citrus fruit, has been found to have potential health benefits such as antioxidation and anti-inflammation activities, lipid metabolism improvement, neuroprotection, and body weight regulation.[2] Nevertheless, it is associated with interactions with certain drugs including calcium channel blockers, immunosuppressants, and antihistamines, which is a well-known food−drug interaction named the "GF juice effect".[3] According to the principles of pharmaphylogeny and phytochemistry, plants that belong to the same family and genus tend to have similar chemical compositions.[4] Especially, the distribution of coumarins and furanocoumarins that are related to the GF juice effect in citrus species closely matches citrus phylogeny.[5] Given this, citrus herbs (CHs), common components in quantities of herbal formulae, probably share various active compounds with GF. CHs are most frequently used for *qi*-regulating based on the theory of traditional Chinese medicine, and the most common ones include *Chenpi* (Pericarpium Citri Reticulatae, PCR), *Qingpi* (Pericarpium Citri Reticulatae Viride, PCRV), *Zhike* (Fructus Aurantii, FA), *Zhishi* (Fructus Aurantii Immaturus, FAI), *Juhong* (Exocarpium Citri Rubrum, ECR), *Huajuhong* (Exocarpium Citri Grandis, ECG), *Xiangyuan* (Fructus Citri, FC), and *Foshou* (Fructus Citri Sarcodactylis, FCS). Owing to

Received: July 20, 2022
Accepted: September 20, 2022
Published: September 29, 2022

https://doi.org/10.1021/acsomega.2c04579
ACS Omega 2022, 7, 35911−35923

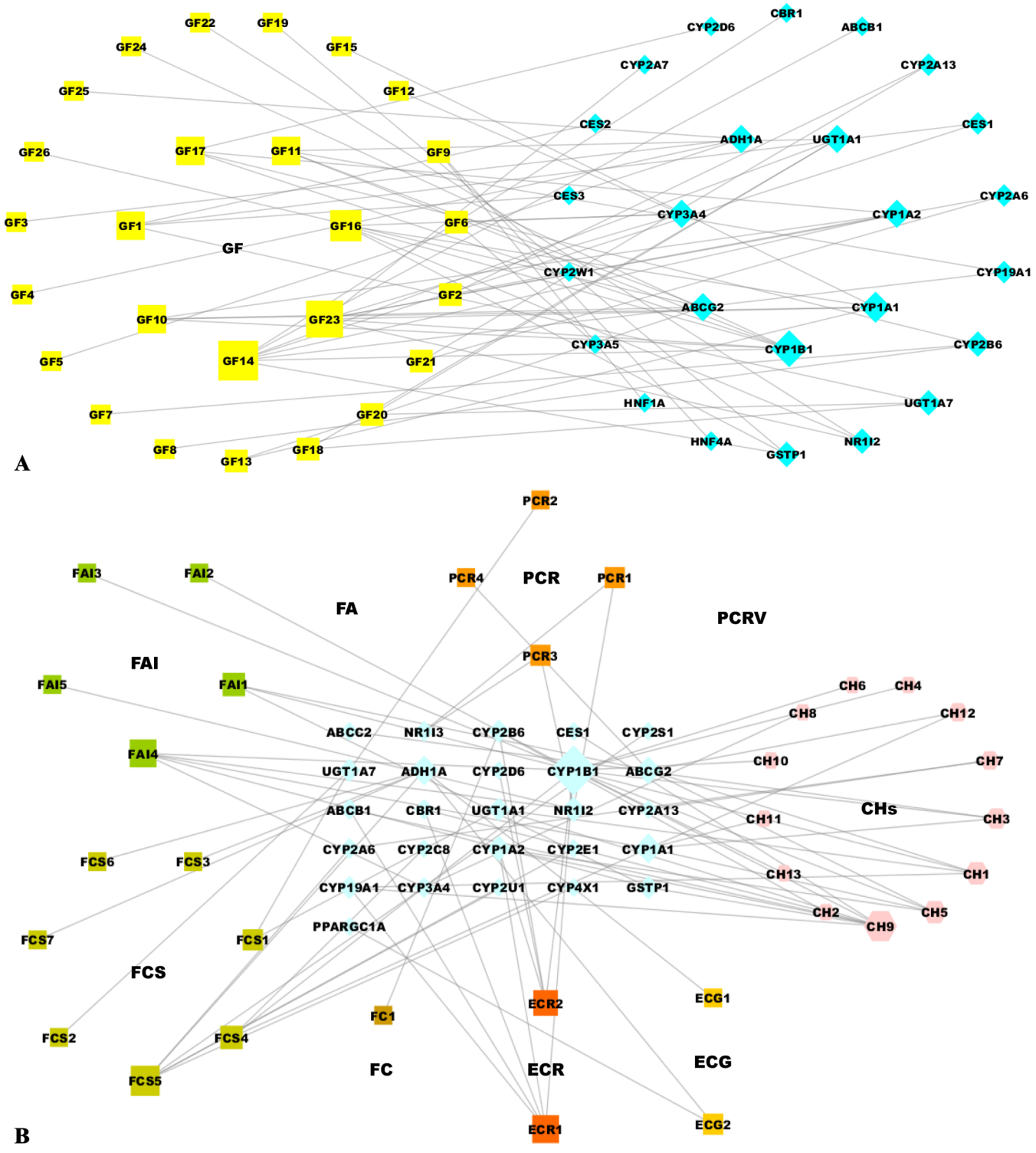

Figure 1. GF (A) and CH (B) compound−target networks related to drug transport and metabolism.

their wide pharmacological effects on the cardiovascular, digestive, and respiratory systems, they have been used commonly in clinical practice to treat diseases involving multiple systems.[6] However, they have the potential to induce HDIs alike the GF juice effect due to their similar chemical compositions. It was once reported that Fructus Citrus maxima induced a 1.5-fold increase in the blood level of tacrolimus in a renal transplant patient.[7]

Network pharmacology is a paradigm shift in pharmaceutical discovery, which is hopeful of deciphering the drug mechanism with a holistic perspective. The research paradigm has shifted from the "one drug for one target" mode to a "multiple components for network targets" mode.[8] Apparently, the principles of network pharmacology are applicable to the phenomena of the GF juice effect and HDIs, involving multiple components and targets. To predict complicated HDIs of CHs, network analysis was employed in this research. Molecular

https://doi.org/10.1021/acsomega.2c04579
ACS Omega 2022, 7, 35911−35923

Table 1. GF and CH Compounds Associated with Drug Transport and Metabolism

GF compounds associated with drug transport and metabolism				CH compounds associated with drug transport and metabolism				
ID	PubChem CID	chemical name	molecular formula	ID	PubChem CID	chemical name	molecular formula	CH sources
GF1	4133	methyl salicylate	$C_8H_8O_3$	CH1	5280443	apigenin	$C_{15}H_{10}O_5$	FAI, ECR, ECG
GF2	798	indole	C_8H_7N	CH2	637566	geraniol	$C_{10}H_{18}O$	ECR, ECG, FC
GF3	998	phenylacetaldehyde	C_8H_8O	CH3	3314	eugenol	$C_{10}H_{12}O_2$	FAI, ECG
GF4	8794	phenylacetonitrile	C_8H_7N	CH4	42607889	5,7,3′-trihydroxy-5′-methoxyflavanone	$C_{16}H_{14}O_6$	PCRV, FAI, ECR, ECG, FA, PCR
GF5	6054	2-phenylethanol	$C_8H_{10}O$	CH5	145659	sinensetin	$C_{20}H_{20}O_7$	PCRV, FAI, ECG, PCR
GF6	2758	eucalyptol	$C_{10}H_{18}O$	CH6	72281	hesperetin	$C_{16}H_{14}O_6$	FA, FC, ECG
GF7	637566	geraniol	$C_{10}H_{18}O$	CH7	5281426	umbelliferone	$C_9H_6O_3$	ECR, ECG
GF8	638011	citral	$C_{10}H_{16}O$	CH8	179651	limonin	$C_{26}H_{30}O_8$	FAI, ECR, FC, FA, PCR
GF9	5280934	linolenic acid	$C_{18}H_{30}O_2$	CH9	439246	naringenin	$C_{15}H_{12}O_5$	PCR, PCRV, FAI, FA, ECR, ECG
GF10	145659	sinensetin	$C_{20}H_{20}O7$	CH10	676152	5,7-dihydroxy-2-(3-hydroxy-4-methoxyphenyl)chroman-4-one	$C_{16}H_{14}O_6$	PCR, PCRV, FAI
GF11	5280443	apigenin	$C_{15}H_{10}O_5$	CH11	68077	tangeretin	$C_{20}H_{20}O_7$	PCR, PCRV, FAI, ECG, FA
GF12	5280371	bergaptol	$C_{11}H_6O_4$	CH12	72344	nobiletin	$C_{21}H_{22}O_8$	PCR, PCRV, FAI, FA, ECG
GF13	72344	nobiletin	$C_{21}H_{22}O_8$	CH13	1149877	(2*R*)-5,7-dihydroxy-2-(4-methoxyphenyl)-2,3-dihydrochromen-4-one	$C_{16}H_{14}O_5$	FAI, ECG, FC
GF14	439246	naringenin	$C_{15}H_{12}O_5$	ECG1	7362	furfural	$C_5H_4O_2$	ECG
GF15	68077	tangeretin	$C_{20}H_{20}O_7$	ECG2	938	nicotinic acid	$C_6H_5NO_2$	ECG
GF16	68079	isopimpinellin	$C_{13}H_{10}O_5$	ECR1	667495	(2*R*)-5,7-dihydroxy-2-(4-hydroxyphenyl)-2,3-dihydro-4*H*-chromen-4-one	$C_{15}H_{12}O_5$	ECR
GF17	68081	isoimperatorin	$C_{16}H_{14}O_4$	ECR2	68081	isoimperatorin	$C_{16}H_{14}O_4$	EC
GF18	6989	thymol	$C_{10}H_{14}O$	FAI1	5280445	luteolin	$C_{15}H_{10}O_6$	FAI
GF19	16724	*d*-carvone	$C_{10}H_{14}O$	FAI2	10212	imperatorin	$C_{16}H_{14}O_4$	FAI
GF20	5280460	scopoletin	$C_{10}H_8O4$	FAI3	373261	eriodyctiol (flavanone)	$C_{15}H_{12}O_6$	FAI
GF21	5281426	umbelliferone	$C_9H_6O_3$	FAI4	68079	isopimpinellin	$C_{13}H_{10}O_5$	FAI
GF22	1017	phthalic acid	$C_8H_6O_4$	FAI5	631170	3′,4′,5,7-tetramethoxyflavone	$C_{19}H_{18}O_6$	FAI
GF23	4114	methoxsalen	$C_{12}H_8O_4$	FC1	638011	citral	$C_{10}H_{16}O$	FC
GF24	72281	hesperetin	$C_{16}H_{14}O_6$	FCS1	5280460	scopoletin	$C_{10}H_8O_4$	FCS
GF25	15512	3-cyclohexene-1-methanol	$C_7H_{12}O$	FCS2	8468	vanillic acid	$C_8H_8O_4$	FCS
GF26	150893	3,3′,4′,5,6,7,8-heptamethoxyflavone	$C_{22}H_{24}O_9$	FCS3	259994	(*R*)-propane-1,2-diol	$C_3H_8O_2$	FCS
				FCS4	5281612	diosmetin	$C_{16}H_{12}O_6$	FCS
				FCS5	8299	hydroxyacetone	$C_3H_6O_2$	FCS
				FCS6	637497	(*R*)-butane-1,3-diol	$C_4H_{10}O_2$	FCS
				FCS7	220010	meso-2,3-butanediol	$C_4H_{10}O_2$	FCS
				PCR1	6782	diisobutyl phthalate	$C_{16}H_{22}O_4$	PCR
				PCR2	1183	vanillin	$C_8H_8O_3$	PCR
				PCR3	6781	diethyl phthalate	$C_{12}H_{14}O_4$	PCR
				PCR4	150893	3,3′,4′,5,6,7,8-heptamethoxyflavone	$C_{22}H_{24}O_9$	PCR

docking and in vitro experiments were also conducted to reveal associations between compounds and targets.

2. RESULTS

2.1. Network Study on the "GF Juice Effect" and HDIs of CHs. A total of 405 and 250 components, respectively, in GF and CHs were identified. Through ADME screening, 249 components in GF and 159 ingredients in CHs exhibited great potential as active compounds, which are listed in Table S1. As for targets, a total of 360 genes related to 141 compounds in GF were collected via public databases for target prediction, while 422 genes were linked to 125 compounds in CHs.

Through the retrieval from the NCBI Gene database, 111 genes associated with drug transport and metabolism were obtained. The results of the Venn diagram suggested that 25 and 26 overlapping genes were identified by matching 360 GF-related genes and 422 CHs-related genes, as well as the above genes related to drug transport and metabolism (Figure S1). The majority of GF-related (18/25) and CHs-related (18/26) targets associated with drug transport and metabolism were identical.

The interactions between compounds and targets related to drug transport and metabolism were visualized. As shown in Figure 1A, the compound−target network of GF consisted of 51 nodes (26 compounds and 25 targets) and 62 interacting

https://doi.org/10.1021/acsomega.2c04579
ACS Omega 2022, 7, 35911−35923

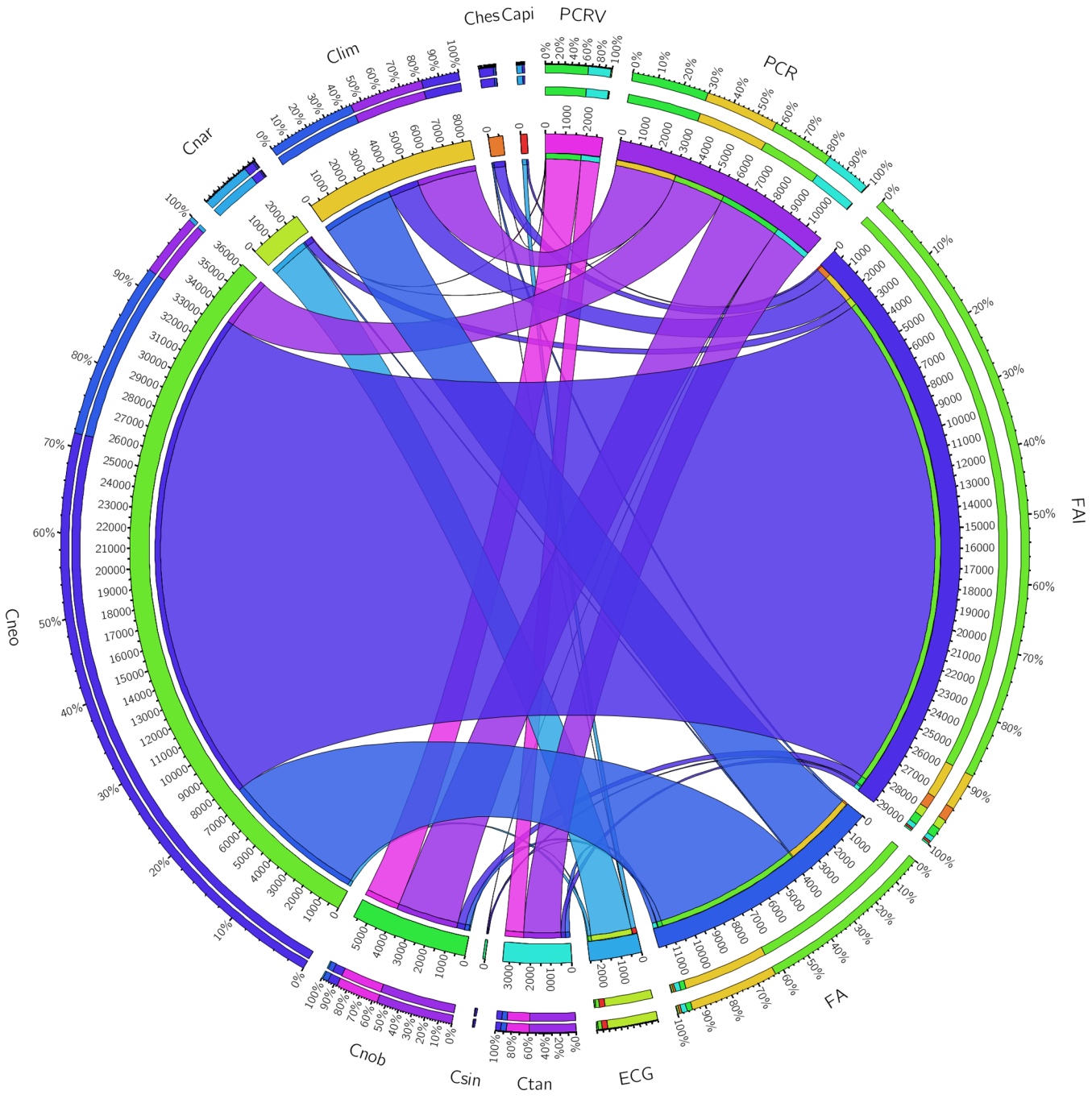

Figure 2. Content distribution (maximum) of typical overlapping compounds in CHs. Note: Capi, apigenin; Ches, hesperetin; Clim, limonin; Cnar, naringenin; Cneo, neohesperidin; Cnob, nobiletin; Csin, sinensetin; Ctan, tangeretin.

edges. Naringenin, methoxsalen, isopimpinellin, methyl salicylate, sinensetin, apigenin, and isoimperatorin had higher degree values, suggesting that they might affect more drug transporters and drug-metabolizing enzymes. Besides, the compound−target network of CHs included 34 compounds' and 26 targets' nodes and 75 edges, which suggested that key compounds with bioactivities including naringenin, hydroxyacetone, isopimpinellin, apigenin, sinensetin, and isoimperatorin were more likely to play a part in drug transport and metabolism (Figure 1B). GF and CHs shared the majority of key compounds, among which naringenin possessed the highest degree value. The more chemical information is summarized in Table 1. Pharmacokinetic prediction results of the compounds via SwissADME are specified in Table S2. The distribution of some typical overlapping CH compounds was retrieved from literature reports. The maximum content was visualized via a chord diagram (Figure 2), while the content (range) is given in Table S3.

Protein−protein interaction (PPI) networks of GF and CH targets related to drug transport and metabolism are depicted in Figure 3. The topological parameters of each target are detailed in Table S4. A total of 24 nodes and 142 edges were involved in the GF PPI network, of which the top seven targets included UGT1A1, CYP3A4, UGT1A7, NR1I2, CYP2B6, CYP1A1, and CYP3A5. All of the targets and their related drugs (examples) are listed in Table S5. The CH PPI network

https://doi.org/10.1021/acsomega.2c04579
ACS Omega 2022, 7, 35911−35923

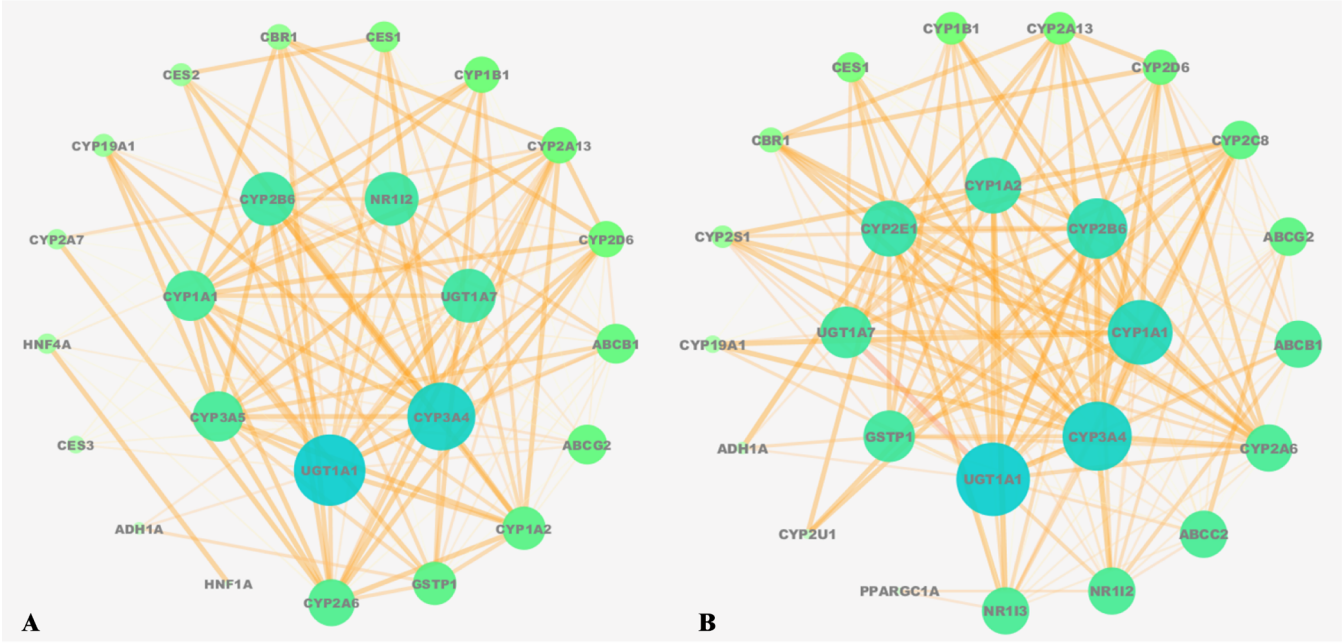

Figure 3. PPI networks of GF (A) and CH (B) targets related to drug transport and metabolism.

included 25 nodes and 170 edges, in which UGT1A1, CYP3A4, CYP1A1, CYP2B6, CYP1A2, CYP2E1, UGT1A7, and GSTP1 were considered as hub targets, as listed in Table S5 together with their related drugs (examples). Pharmacokinetic pathways of some typical related drugs are displayed in Figure S2. The importance of 18 mutual genes differed in the PPI network of GF and CHs, except for the top two targets, namely, UGT1A1 and CYP3A4.

Remarkably, multiple chemical components might interact with various drugs via diverse targets. Some key compounds served as examples below. Caffeine, clopidogrel, etoposide, tamoxifen, theophylline, and verapamil were linked to naringenin with the aid of ABCB1, CBR1, CES1, CYP1A2, CYP1B1, CYP19A1, GSTP1, and UGT1A1. Isopimpinellin might affect CYP1A1, CYP1B1, CYP3A4, GSTP1, and NR1I2, and therefore influence the pharmacokinetics of drugs such as erlotinib, nilotinib, paclitaxel, tamoxifen, and verapamil. Apigenin was associated with the regulation of ABCG2, CYP1B1, CYP19A1, and UGT1A1 and might interact with etoposide and tamoxifen consequently. Potential interactions of sinensetin with caffeine and theophylline were probably mediated by ABCG2, CYP1A1, CYP1A2, and CYP1B1. Isoimperatorin might influence the metabolism of caffeine, tamoxifen, theophylline, and venlafaxine, which was possibly related to its effect on CYP1A2, CYP1B1, CYP2B6, and CYP2D6.

The mutual compounds of GF and CHs were identified with the aid of chemical structures. GF and CHs shared 48 potential active compounds (Table 2). As shown in Figure 4A, 43 compounds were related to 262 target genes, which formed 650 interaction edges. In the network, naringenin, tangeretin, nobiletin, and apigenin possessed more connections with targets.

Gene Ontology (GO) enrichment analysis results of mutual targets are shown in Figure 4, which included biological processes (top 5%, Figure 4B), cellular components (top 10%, Figure 4C), and molecular functions (top 10%, Figure 4D). Biological processes (including response to drug, oxidation−reduction process, and negative regulation of the apoptotic process) cellular components (including the plasma membrane, integral component of the membrane, and cytosol), and molecular functions (including protein binding, enzyme binding, and protein homodimerization) manifested themselves. The results of the Kyoto Encyclopedia of Genes and Genomes (KEGG) pathway enrichment analysis indicated that 285 mutual targets were significantly enriched in 149 signaling pathways ($P < 0.05$). The top 20 signaling pathways are shown in Figure 4E. Apart from the pathways of multiple diseases, the metabolism of xenobiotics by cytochrome P450 and cytochrome P450 drug metabolism demonstrated significance.

2.2. Molecular Docking of Mutual Compounds and Target Proteins. The details of docking results are listed in Table 3. The results showed that apigenin had the best docking effect with UGT1A1, while nobiletin had the greatest binding potential with CYP3A4. The three-dimensional (3D) diagrams of molecular docking models are displayed in Figure 5, which showed the binding mode and sites between each compound and protein.

2.3. In Vitro Tests on the Potential Common Mechanism of the "GF Juice Effect" and HDIs of CHs. Concentration−cell viability curves of the four flavonoids via the CCK-8 assay are provided in Figure S3. Accordingly, the corresponding tested concentrations were selected: naringenin, 10 μmol·L^{-1}; tangeretin, 10 μmol·L^{-1}; nobiletin 20 μmol·L^{-1}; and apigenin, 1 μmol·L^{-1}. As shown in Figure 6, the UGT1A1 activity of HepG2 cells was significantly raised by naringenin and tangeretin, while nobiletin and apigenin demonstrated different degrees of ability to decrease it. Meanwhile, the western blot test indicated that the CYP3A4 expression of the cells tended to be reduced by the four compounds.

3. DISCUSSION

In this research, it was predicted that various drugs might be affected in pharmacokinetics by GF and CHs. In fact, there was a growing body of evidence for the "GF juice effect". The interactions between GF and the majority of the predicted

https://doi.org/10.1021/acsomega.2c04579
ACS Omega 2022, 7, 35911−35923

Table 2. Mutual Compounds of GF and CHs[a]

ID	PubChem CID	chemical name	molecular formula	CH sources
C1	5280443	apigenin	$C_{15}H_{10}O_5$	FAI, ECR, ECG
C2	5280460	scopoletin	$C_{10}H_8O_4$	FCS
C3	985	palmitic acid	$C_{16}H_{32}O_2$	ECG, FCS
C4	8175	decanal	$C_{10}H_{20}O$	PCR, FC
C5	637566	geraniol	$C_{10}H_{18}O$	ECR, ECG, FC
C6	638011	citral	$C_{10}H_{16}O$	FC
C7	443158	(−)-linalool	$C_{10}H_{18}O$	PCR, PCRV, ECR, ECG, FC
C8	3893	lauric acid	$C_{12}H_{24}O_2$	PCR, FCS
C9	1549025	neryl acetate	$C_{12}H_{20}O_2$	PCR
C10	8748	β-terpineol	$C_{10}H_{18}O$	PCR
C11	643820	nerol	$C_{10}H_{18}O$	FCS
C12	5325830	(−)-terpinen-4-ol	$C_{10}H_{18}O$	PCR, FCS
C13	637531	pichtosin	$C_{12}H_{20}O_2$	FCS
C14	11005	myristic acid	$C_{14}H_{28}O_2$	ECG, FCS
C15	13849	pentadecanoic acid	$C_{15}H_{30}O_2$	ECG
C16	145659	sinensetin	$C_{20}H_{20}O_7$	PCRV, FAI, ECG, PCR
C17	68081	isoimperatorin	$C_{16}H_{14}O_4$	ECR
C18	2355	bergapten	$C_{12}H_8O_4$	FAI, ECR, ECG
C19	8417	scoparone	$C_{11}H_{10}O_4$	FCS
C20	1742210	caryophyllene oxide	$C_{15}H_{24}O$	ECG
C21	8892	hexanoic acid	$C_6H_{12}O_2$	FCS
C22	72281	hesperetin	$C_{16}H_{14}O_6$	FA, FC, ECG
C23	7793	(−)-citronellol	$C_{10}H_{20}O$	FC
C24	5281426	umbelliferone	$C_9H_6O_3$	ECR, ECG
C25	6428300	trans-(+)-pyranoid linalool oxide	$C_{10}H_{18}O_2$	PCR
C26	8158	nonanoic acid	$C_9H_{18}O_2$	ECG
C27	68079	isopimpinellin	$C_{13}H_{10}O_5$	FAI
C28	6826	methyl 2-(methylamino)benzoate	$C_9H_{11}NO_2$	PCR
C29	8635	methyl anthranilate	$C_8H_9NO_2$	ECG
C30	439246	naringenin	$C_{15}H_{12}O_5$	PCR, PCRV, FAI, FA, ECR, ECG
C31	2775	5,7-dimethoxycoumarin	$C_{11}H_{10}O_4$	FC, FCS
C32	443178	(+)-trans-carveol	$C_{10}H_{16}O$	FCS
C33	8186	undecanal	$C_{11}H_{22}O$	PCR
C34	150893	3,3′,4′,5,6,7,8-heptamethoxyflavone	$C_{22}H_{24}O_9$	PCR
C35	68077	tangeretin	$C_{20}H_{20}O_7$	PCR, PCRV, FAI, ECG, FA
C36	5281534	α-sinensal	$C_{15}H_{22}O$	PCR
C37	72344	nobiletin	$C_{21}H_{22}O_8$	PCR, PCRV, FAI, FA, ECG
C38	9727	*N*-methyltyramine	$C_9H_{13}NO$	FAI, FA, FC
C39	5284503	3-hexen-1-ol	$C_6H_{12}O$	ECG
C40	629964	4′,5,7,8-tetramethoxyflavone	$C_{19}H_{18}O_6$	FAI, ECG
C41	854067	(−)-synephrine	$C_9H_{13}NO_2$	FA, FC
C42	6450230	marmin	$C_{19}H_{24}O_5$	FA
C43	1550607	auraptene	$C_{19}H_{22}O_3$	FAI
-	643779	neral	$C_{10}H_{16}O$	PCR, PCRV, ECR, ECG, FCS
-	1549026	geranyl acetate	$C_{12}H_{20}O_2$	FC
-	454	octanal	$C_8H_{16}O$	PCR, FC
-	5283361	2-dodecenal	$C_{12}H_{22}O$	PCR
-	8174	1-decanol	$C_{10}H_{22}O$	PCR

[a]Note: ID "-" means that no target genes related to the compound were obtained.

related drugs in this research were reported in clinical studies, and the clinical evidence mainly focused on pharmacokinetic interactions. In general, there were mainly two opposite situations. One was that GF can lessen plasma exposure to certain drugs such as etoposide, which may diminish curative effects.[3] The other condition was that plasma exposure to certain drugs was increased, which may enhance curative effects or trigger off side effects.[9] Psychotropic drugs (caffeine, midazolam), cardiovascular drugs (nifedipine, verapamil), immunosuppressive agents (cyclosporine), antineoplastic drugs (nilotinib), antiepileptic drugs (carbamazepine), antidepressant drugs (sertraline), analgesic drugs (methadone), and antifungal agents (itraconazole) were involved in such "GF juice effect".[3] There also existed some experimental evidence for HDIs of CHs, which certainly fell far behind that for the "GF juice effect". Pomelo peel, a source of CGE, was found to significantly increase the bioavailability of cyclosporine and tacrolimus in rats.[10] FAI decreased the bioavailability of tacrolimus in rats, while FA showed no remarkable effect.[11]

https://doi.org/10.1021/acsomega.2c04579
ACS Omega 2022, 7, 35911−35923

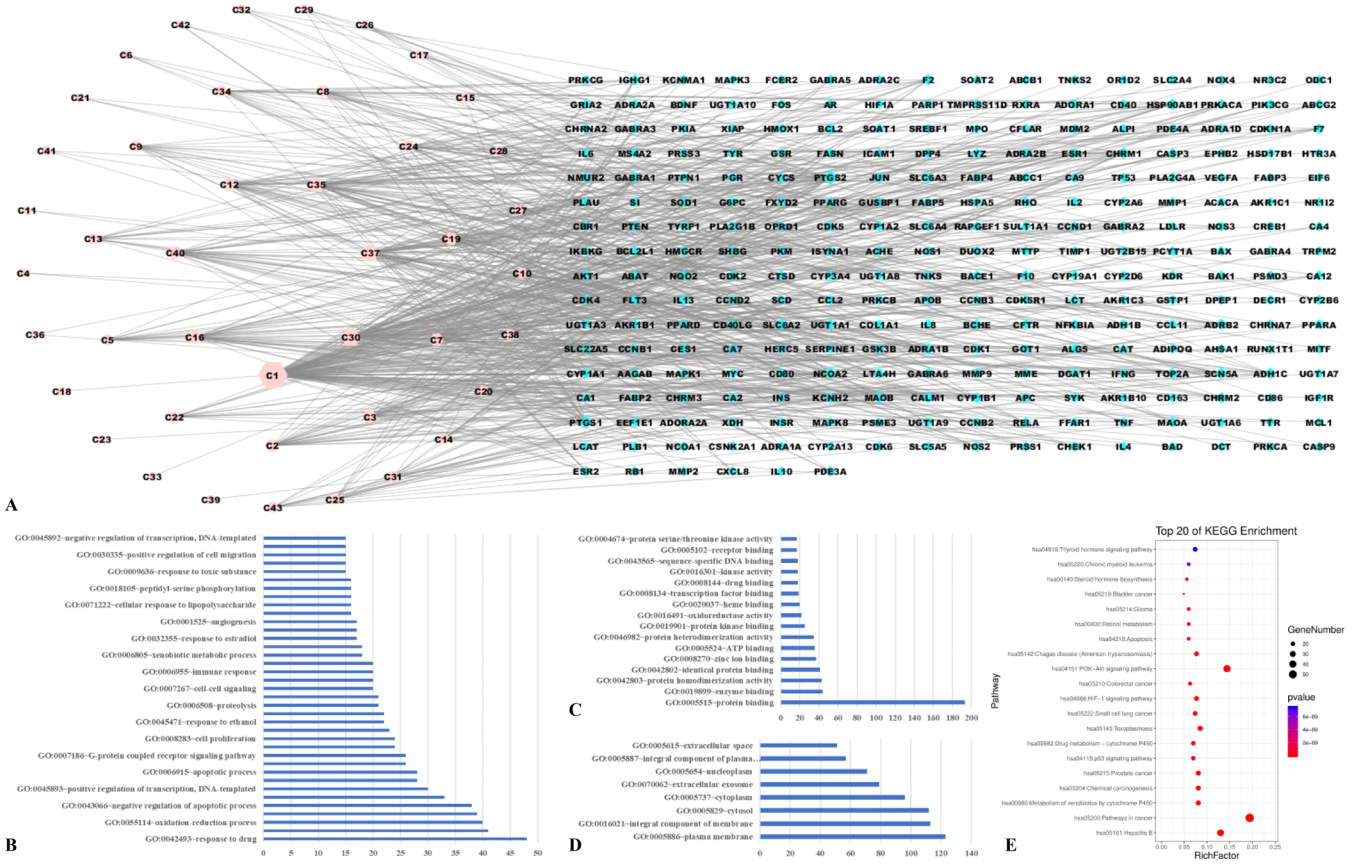

Figure 4. Network and enrichment analysis of mutual targets. (A) Mutual compound−target network of GF and CHs. (B) Gene Ontology (GO) enrichment analysis (biological process, BP) results of mutual targets. (C) GO enrichment analysis (molecular function, MF) results of mutual targets. (D) GO enrichment analysis (cellular component, CC) results of mutual targets. (E) KEGG pathway analysis results of mutual targets.

Table 3. Docking Results of Mutual Compounds and Target Proteins

target protein	compound type	compound name	lowest binding energy/kcal·mol^{-1}	inhibiting constant/μmol·L^{-1}	number of hydrogen bonds	number of hydrophobic interactions
UGT1A1	inhibitor	dacomitinib	−6.61	14.32	1	5
	inducer	phenobarbital	−5.1	182.12	5	3
	tested compound	naringenin	−5.41	107.37	3	6
	tested compound	tangeretin	−4.87	268.93	1	3
	tested compound	nobiletin	−3.9	1380	3	3
	tested compound	apigenin	−5.48	96.34	3	2
CYP3A4	inhibitor	ketoconazole	−7.64	2.52	3	4
	inducer	phenobarbital	−6.81	10.21	3	4
	tested compound	naringenin	−6.92	8.53	6	3
	tested compound	tangeretin	−5.89	48.21	3	2
	tested compound	nobiletin	−7.05	6.78	5	1
	tested compound	apigenin	−6.86	9.42	5	2

As for the mechanism, it was widely believed that GF influenced drug-metabolizing enzymes, including cytochrome P450 (CYP450) and UDP-glucuronosyltransferase (UGT), and drug transporters such as P-glycoprotein (P-gp) and organic anion transporting polypeptide (OATP) to disturb pharmacokinetics of certain drugs.[12−15] Given the similar material basis, CHs might be associated with regulating these targets. In this research, UGT1A1 and CYP3A4 were predicted to be hub genes of the "GF juice effect" and HDIs of CHs. Moreover, drug metabolism by CYP450 was also regarded as an important pathway. The regulating effects of the key compounds, which included naringenin, tangeretin, nobiletin, and apigenin, on UGT1A1 and CYP3A4 were also preliminarily observed in vitro. In fact, some recent studies

https://doi.org/10.1021/acsomega.2c04579
ACS Omega 2022, 7, 35911−35923

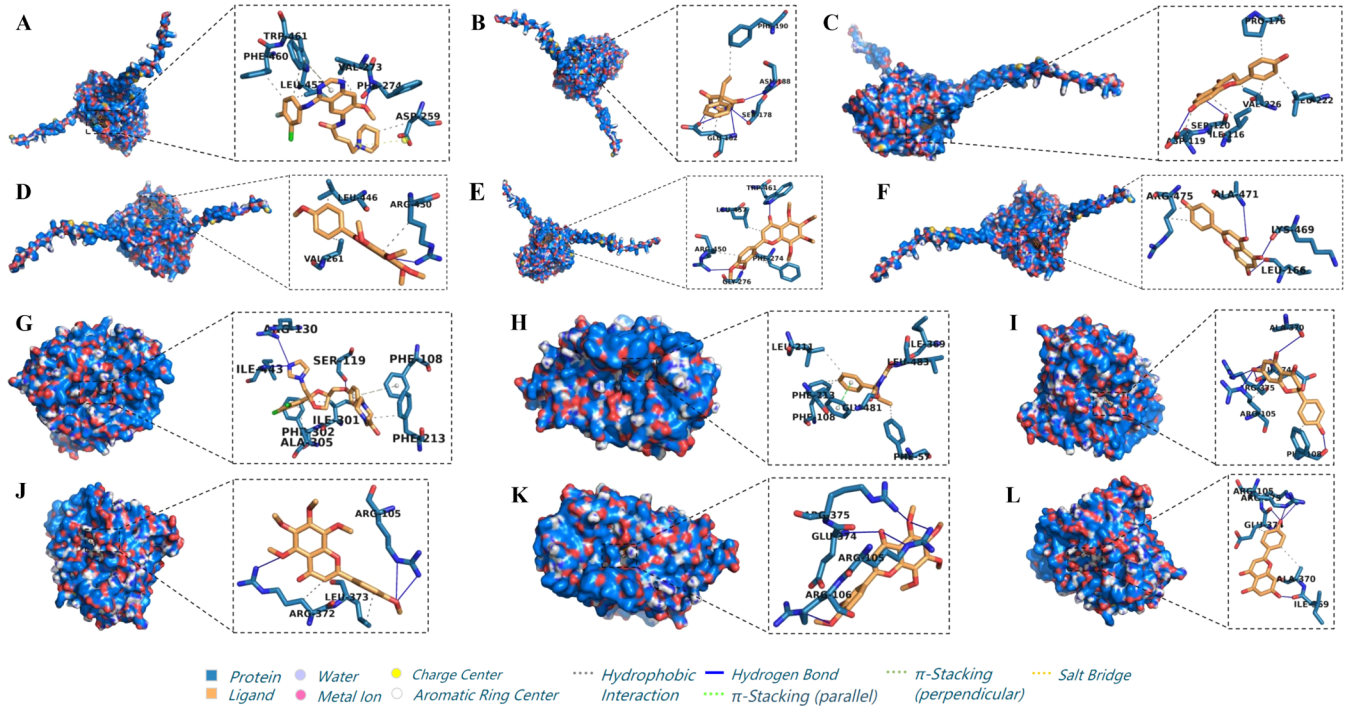

Figure 5. Binding mode of mutual compounds and target proteins. (A) Dacomitinib and UGT1A1, (B) phenobarbital and UGT1A1, (C) naringenin and UGT1A1, (D) tangeretin and UGT1A1, (E) nobiletin and UGT1A1, (F) apigenin and UGT1A1, (G) ketoconazole and CYP3A4, (H) phenobarbital and CYP3A4, (I) naringenin and CYP3A4, (J) tangeretin and CYP3A4, (K) nobiletin and CYP3A4, and (L) apigenin and CYP3A4.

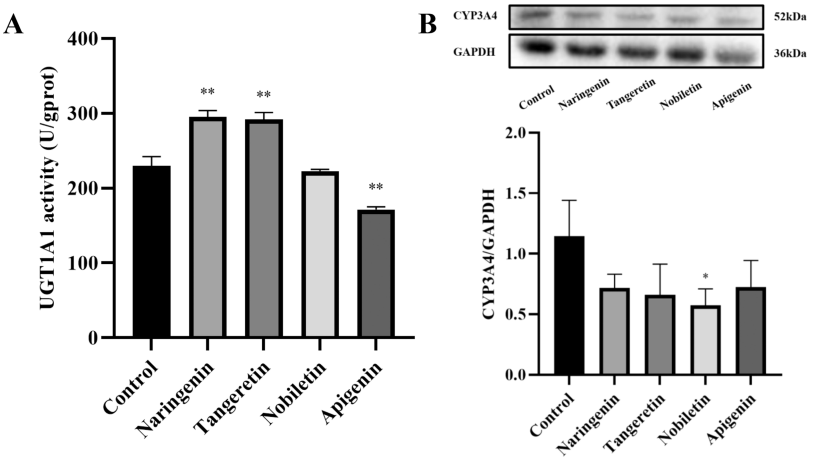

Figure 6. UGT1A1 activity (A) and CYP3A4 expression (B) of HepG2 cells after treatment with naringenin, tangeretin, nobiletin, and apigenin. $n = 3$, * $P < 0.05$, ** $P < 0.01$ versus control group.

focused on the capability of the compounds to regulate the drug-metabolizing enzymes, although the action tendency might be reversed due to different experimental systems and conditions.[15−19] As widely known, CYP450 played a pivotal role in drug metabolism, since the majority of hepatically cleared drugs depended on CYP450 for metabolism.[20] GF inhibited intestinal and hepatic CYP3A4 in an exposure-dependent fashion, and patients taking CYP3A4 substrates are at risk of developing drug-related adverse events if consuming large amounts of GF.[21] The GF-induced pharmacokinetic change of multiple drugs might be better explained by the impairment of CYP450 in the intestinal wall rather than in the liver.[22,23] In rats, FA upregulated the protein expression of CYP1A2, CYP3A4, and CYP2E1 and the mRNA expression of CYP1A2 and CYP3A4, which indicated that it might be a slight inducer of CYP1A2 and CYP3A4.[24] Besides, the extracts of FA and FAI showed mild inhibition on CYP3A.[25] UGTs were a series of enzymes responsible for conjugative phase II reactions of drugs.[26] A cross-sectional study suggested that the intake of citrus fruits including GF might promote UGT1A1 activity among women with a certain genotype.[27] Transporters including P-gp and OATP were often expressed in tissues related to drug disposition concerning intestinal absorption, uptake into hepatocytes, and renal/bile excretion of drugs.[28] GF showed bidirectional effects on P-gp in rats. On the one hand, it inhibited P-gp-mediated drug efflux in cotreatment, but on the other hand, its chronic administration led to increased levels of P-gp expression.[29] A study indicated that

https://doi.org/10.1021/acsomega.2c04579
ACS Omega 2022, 7, 35911−35923

FAI and PCR extracts increased P-gp and CYP3A4 expression via upregulation of the pregnane X receptor in vitro.[30] GF inhibited human enteric OATP1A2 in vitro.[31] The interaction of GF with fexofenadine only at therapeutic concentrations might be better explained as the presence of multiple binding sites on OATP2B1.[32]

There had been some studies paying attention to the exposure dose and duration of the "GF juice effect". A human study confirmed that GF−dextromethorphan pharmacokinetic interaction was dose-dependent and indicated 200 mL of single-strength GF juice as the "lowest observed effect level".[33] It was observed that the recovery of GF-induced enteric CYP3A impairment was largely completed within 3 days, consistent with enzyme regeneration after mechanism-based inhibition.[22] The dose−effect relationship and recovery time for HDIs of CHs remained to be explored further.

In regard to vital compositions in these reactions, multiple furocoumarins and flavonoids showed great potential to cause these interactions. Certain furocoumarins in GF exhibited as strong inhibitors of CYP3A4.[34] Bergamottin was observed to equally increase the absorption of nifedipine in rats by comparison with GF, suggesting that bergamottin played a vital role in GF−nifedipine interaction.[35] In vitro, 6′,7′-dihydroxybergamottin was verified as a potent mechanism-based inhibitor of midazolam α-hydroxylation by CYP3A.[22] These two major furanocoumarins in GF differed in intestinal CYP3A4 inhibition kinetic and binding properties. With human intestinal microsomes, 6′,7′-dihydroxybergamottin was a substrate-independent reversible and mechanism-based inhibitor of CYP3A4. In contrast, bergamottin was a substrate-dependent reversible inhibitor but a substrate-independent mechanism-based inhibitor.[36] Last but not least, the role of GF−CH mutual compounds could not be ignored in these interactions. In vitro naringin was a potent competitive inhibitor of caffeine 3-demethylation dependent on CYP1A2.[37] Potent inhibition of CYP3A4 and negligible inhibitory effects on P-gp and other CYP450 by limonin was observed in vitro.[38] Hesperetin and naringenin exhibited strong inhibition on UGT1A1, while UGT1A7 was moderately inhibited.[15] Molecular docking analysis identified favorable binding of nobiletin with the transmembrane region site 1 of homology modeled human ABCB1 transporter, while in vitro experiment demonstrated that nobiletin profoundly inhibited ABCB1 transporter activity.[39]

This research had some limitations as below, whereas our findings interpreted that some drugs were ultimately connected with CHs by means of network pharmacology. First, CHs and GF differed in usage and dosage. GF juice was more popular, and several hundred milliliters of it might be consumed as a drink habitually. In contrast, CHs were usually used with other herbs in the form of decoctions, and the daily dosage was merely several grams. Second, it was reported that furanocoumarins played a crucial role in the "GF juice effect", and they did not seem so important in the prediction yet. It might be affected by the online databases for component collection and target prediction. Third, this research was specifically aimed at pharmacokinetic interactions instead of pharmacodynamic ones. Moreover, it should be noted that multiple active compounds in CHs varied in content according to diverse factors including species, places of production, collecting time, storage, processing, and preparation, which was bound to have a significant impact on HDIs. The content of GF−CH mutual compounds also remained to be further determined and compared in light of the close connection between dosage and effect.

4. CONCLUSIONS

In the current study, based on network pharmacology, the potential HDIs of CHs were predicted compared with GF, in which diverse conventional drugs were associated with multiple components and targets. Furthermore, molecular docking and in vitro experiments demonstrated that the regulating effects of flavonoids including naringenin, tangeretin, nobiletin, and apigenin on UGT1A1 and CYP3A4 might play a crucial part in HDIs of CHs. Besides, it would benefit from more evidence of clinical practice and scientific experiments in the future.

5. MATERIALS AND METHODS

5.1. Network Study on the "GF Juice Effect" and HDIs of CHs. *5.1.1. Chemical Composition Collection and Screening of GF and CHs.* The Plant Chemical Component Database (http://www.organchem.csdb.cn/scdb/main/plant_introduce.asp), which belonged to the Chemistry Database provided by Shanghai Institute of Organic Chemistry,[40] and the Traditional Chinese Medicine Systems Pharmacology Database and Analysis Platform (TCMSP, https://tcmspw.com/tcmsp.php) were, respectively, employed to identify the chemical components of GF and CHs including ECG, ECR, FA, FAI, FC, FCS, PCR, and PCRV.[41] The canonical SMILES and molecular formulas of all involved components were obtained from PubChem at https://pubchem.ncbi.nlm.nih.gov/ with the aid of chemical names or structures. PubChem is a public database for chemical structures of small molecules, which is conducive to chemical structure standardization.[42]

To obtain compounds with higher oral bioavailability, all components were screened via SwissADME (http://www.swissadme.ch/) with the aid of canonical SMILES. SwissADME is a tool to evaluate the pharmacokinetics and drug-likeness of small molecules.[43] The majority of oral components exhibited bioactivities when absorbed by the gastrointestinal tract, and drug-likeness was a qualitative concept designed to estimate solubility and permeability.[44] Given this, components were selected as potential active compounds when the results of predicted gastrointestinal absorption were high and the output of five drug-likenesses filters (Lipinski, Ghose, Veber, Egan, and Muegge) contained no less than two "Yes".

5.1.2. Collection of Potential Targets. The targets corresponding to the potential active compounds of GF and CHs were acquired from TCMSP. Meanwhile, the canonical SMILES of each compound was imported into SwissTargetPrediction (http://www.swisstargetprediction.ch/) and STITCH (http://stitch.embl.de/), and the species was confined as "*Homo sapiens*", while the required probability was screened as no less than 0.700 to predict the targets of compounds.[45] With regard to STITCH prediction, the compound with the highest Tanimoto score, usually 1.000 (match via InChIKey), was chosen, and the target would be included when its score was no lower than 0.700.[46] Then the targets related to the compounds of GF and CHs were ultimately converted into official gene symbols after being retrieved from UniProt (https://www.uniprot.org/) with the species selected as *H. sapiens*, while the duplicate targets and the compounds with vacant targets were removed ultimately.

https://doi.org/10.1021/acsomega.2c04579
ACS Omega 2022, 7, 35911−35923

Genes related to drug transport and metabolism were collected in the NCBI Gene database (https://www.ncbi.nlm.nih.gov/gene/) with keywords "drug transport", "drug transmembrane transport", "drug metabolism", "drug metabolic", and organism selected as *H. sapiens*. Venny 2.1.0 (http://bioinfogp.cnb.csic.es/tools/venny/index.html) was used to analyze the intersections of GF and CH targets with targets related to drug transport and metabolism.[47]

5.1.3. Compound−Target Network Construction and Analysis. Based on the data previously collected, compound−target networks associated with drug transport and metabolism were illustrated via Cytoscape 3.7.1, a network visualization and analysis software.[48] Degree values provided by NetworkAnalyzer, a tool of Cytoscape, were adopted for the importance of compound nodes in the network. In addition, taking multiple compounds shared by CHs into consideration, the content of typical overlapping CH compounds was retrieved from literature reports to compare and contrast the herbs. The compound content (range) was collected, and the maximum content was visualized via Circos Table Viewer v0.63−9 (http://mkweb.bcgsc.ca/tableviewer/visualize/).[49] Furthermore, since GF and CHs shared diverse chemical components, the mutual compounds were checked and the compound−target network was also constructed to seek their common composition that might play a significant role.

5.1.4. Protein−Protein Interaction Analysis. STRING ver.11.0 (https://string-db.org/) was utilized to conduct PPI for the selected targets, which was an online database providing associations between proteins based on curated databases, experimentally determined, gene neighborhood, gene fusions, gene co-occurrence, text mining coexpression, and protein homology. In the process, the species was limited to *H. sapiens*, and the minimum required interaction score was selected as medium confidence (0.400).[50] Disconnected nodes in the PPI network were hidden. The visualization of PPI was optimized through Cytoscape. Afterward, three topological parameters including degree, between centrality, and close centrality of each target were analyzed to describe influential nodes in the PPI network.

5.1.5. Collection of Related Drugs and Their Pathways. To provide information on the potential interactions of GF and CHs with certain drugs, DrugBank (https://www.drugbank.ca/), a database that combined detailed drug data with comprehensive drug target information, was adopted to gain related drugs of target genes.[51] Moreover, pathways of the drug above were collected via the Pharmacogenomics Knowledge Base (https://www.pharmgkb.org/), a resource that collected, curated, and disseminated information concerning human genetic variation on drug responses.[52]

5.1.6. Gene Ontology and Pathway Enrichment Analysis of Mutual Targets. To interpret the potential mechanism of the mutual targets linked to GF and CHs, Database for Annotation, Visualization, and Integrated Discovery (https://david.ncifcrf.gov/) 6.8 was utilized for GO and KEGG pathway enrichment analysis with the species setting of *H. sapiens*.[53,54] GO analysis included the aspects of the biological process (BP), molecular function (MF), and cellular component (CC). The *P*-value was calculated in the enrichment analyses, and $P < 0.05$ indicated that the enrichment degree was statistically significant. The results were visualized as a bubble chart via OmicShare tools (http://omicshare.com/).

5.2. Molecular Docking Simulations. Simulations were conducted between the top two target proteins and four typical mutual compounds of CHs and GF. The 3D structure of the target proteins was obtained from the Protein Data Bank (https://www.rcsb.org/) and the AlphaFold Protein Structure Database (https://alphafold.ebi.ac.uk/).[55,56] Target protein preparation including removing the solvent molecules and the original ligands was performed through PyMOL, while the structure of the compounds was collected from PubChem.[42] Then, molecular docking was performed with AutoDock 4.2.6 software. A total of 50 independent docking runs were conducted for each compound and target protein. The best docking model with the lowest binding energy was selected as the optimal model and used to demonstrate the binding mode and sites. The Protein−Ligand Interaction Profiler (https://plip-tool.biotec.tu-dresden.de/plip-web/plip/index) was utilized to analyze the docking results,[57] and visualization was completed with PyMOL. Meanwhile, a definite inhibitor and an inducer of the targets were chosen to be docked for a comparison.

5.3. In Vitro Tests. *5.3.1. Cell Culture.* Human hepatoma-derived HepG2 cells, generously provided by Prof. Jian Ni (Beijing University of Chinese Medicine, Beijing, China), were cultivated in Dulbecco's modified Eagle's medium (DMEM) (Gibco) supplemented with 10% fetal bovine serum (Analysis Quiz, China) and 1% penicillin−streptomycin (Gibco) at 37 °C in a 5% CO_2 atmosphere. In vitro experiments were performed using HepG2 cells between passages 15 and 20, which were subcultured at approximately 80% confluence.

5.3.2. Cell Viability Assay. HepG2 cells (4000 per well) were cultured into 96-well plates for 24 h, and they were exposed to a series of concentrations of naringenin, nobiletin, apigenin (Shanghai Yuanye Bio-Technology Co., Ltd, China), and tangeretin (Shanghai Standard Technology Co., Ltd., China) for another 24 h. A cell counting kit-8 (CCK-8) solution (Biorigin Inc., China) assay was conducted to screen the safety concentrations of the four compounds on HepG2 cells. The concentration−cell viability curves were drawn, and half of the value of the concentration when cell viability reached 90% was considered as the tested concentration, at which cell viability was expected to be over 85% in another assay.

5.3.3. Enzyme-Linked Immunosorbent Assay of UGT1A1. The concentration of UGT1A1 in HepG2 cells was determined using human UGT1A1 enzyme-linked immunosorbent assay (ELISA) kits (Jiangsu Meibiao Biotechnology Co., Ltd, China) according to the manufacturer's instructions, which took advantage of specific antigen−antibody reactions. Meanwhile, the protein concentrations of the samples were obtained using a BCA Protein Assay Kit (Beijing Solarbio Science & Technology Co., Ltd., China). The UGT1A1 concentration per protein concentration was ultimately calculated for normalization by dividing the UGT1A1 concentration by the total protein concentration.

5.3.4. Western Blot Analysis of CYP3A4. The proteins of HepG2 cells from different groups were harvested and then lysed with cold RIPA buffer (Beijing Solarbio Technology Co., Ltd, China) supplemented with a protease inhibitor cocktail for 20 min on ice. The protein concentrations of the supernatant were measured with a BCA Protein Assay Kit. Next, equal amounts (10 μg) of the protein were separated via precast 10% sodium dodecyl sulfate (SDS)-polyacrylamide gel and transferred onto poly(vinylidene difluoride) (PVDF) membranes (Millipore Inc.). After blocking with TBST buffer containing 5% skim milk for 1 h at room temperature, the

https://doi.org/10.1021/acsomega.2c04579
ACS Omega 2022, 7, 35911−35923

PVDF membranes were incubated overnight at 4 °C with the CYP3A4 antibody (1:6000, Proteintech Group, Inc.), followed by incubation with the appropriate secondary antibody at room temperature for another 1 h. At last, the blots were visualized by SageCapture software (Beijing Sage Creation Science Company, China), the levels of protein expression were normalized to that of GAPDH, and relative protein expression was quantified using ImageJ software (National Institutes of Health).

5.3.5. Statistical Analysis. The statistical analysis of data as mean ± standard deviation was performed by utilizing SPSS software (version 26.0, International Business Machines Corporation). According to the normality- and variance-related data of each group, the one-way analysis of variance (ANOVA) and the Kruskal–Wallis test were applied to indicate a significant difference, which was associated with the P-value < 0.05.

■ ASSOCIATED CONTENT

Supporting Information

The Supporting Information is available free of charge at https://pubs.acs.org/doi/10.1021/acsomega.2c04579.

Potential active compounds of GF and CHs; pharmacokinetic prediction results of compounds via SwissADME; typical overlapping CH compound content (range) from literature reports; topological parameters of GF and CH targets related to drug transport and metabolism; GF and CH targets related to drug transport and metabolism along with the related drugs; overlapping genes among GF genes, CH genes and genes related to drug transport and metabolism; pharmacokinetic pathways of typical related drugs (erlotinib, verapamil, tamoxifen, nilotinib, venlafaxine, and theophylline); and concentration–cell viability curves of mutual compounds on HepG2 cells (PDF)

■ AUTHOR INFORMATION

Corresponding Author

Bing Zhang − *School of Chinese Materia Medica, Beijing University of Chinese Medicine, Beijing 102488, China; Center for Pharmacovigilance and Rational Use of Chinese Medicine, Beijing University of Chinese Medicine, Beijing 102488, China;* orcid.org/0000-0001-6391-5142; Email: zhangb@bucm.edu.cn

Authors

Jintao Lü − *School of Chinese Materia Medica, Beijing University of Chinese Medicine, Beijing 102488, China; Center for Pharmacovigilance and Rational Use of Chinese Medicine, Beijing University of Chinese Medicine, Beijing 102488, China*

Dan Zhang − *School of Chinese Materia Medica, Beijing University of Chinese Medicine, Beijing 102488, China; Center for Pharmacovigilance and Rational Use of Chinese Medicine, Beijing University of Chinese Medicine, Beijing 102488, China*

Xiaomeng Zhang − *School of Chinese Materia Medica, Beijing University of Chinese Medicine, Beijing 102488, China; Center for Pharmacovigilance and Rational Use of Chinese Medicine, Beijing University of Chinese Medicine, Beijing 102488, China*

Rina Sa − *School of Chinese Materia Medica, Beijing University of Chinese Medicine, Beijing 102488, China; Center for Pharmacovigilance and Rational Use of Chinese Medicine, Beijing University of Chinese Medicine, Beijing 102488, China; Gansu Province Hospital, Lanzhou 730000, China*

Xiaofang Wang − *School of Chinese Materia Medica, Beijing University of Chinese Medicine, Beijing 102488, China; Center for Pharmacovigilance and Rational Use of Chinese Medicine, Beijing University of Chinese Medicine, Beijing 102488, China*

Huanzhang Wu − *School of Chinese Materia Medica, Beijing University of Chinese Medicine, Beijing 102488, China; Center for Pharmacovigilance and Rational Use of Chinese Medicine, Beijing University of Chinese Medicine, Beijing 102488, China*

Zhijian Lin − *School of Chinese Materia Medica, Beijing University of Chinese Medicine, Beijing 102488, China; Center for Pharmacovigilance and Rational Use of Chinese Medicine, Beijing University of Chinese Medicine, Beijing 102488, China*

Complete contact information is available at: https://pubs.acs.org/10.1021/acsomega.2c04579

Author Contributions

J.L. and B.Z. conceived and designed this work. J.L., D.Z., and X.Z. wrote the whole manuscript. J.L., D.Z., and X.W. conducted the experimental operation. J.L., X.Z., R.S., and H.Z. collected and analyzed the data. Z.L. and B.Z. revised the whole manuscript. All the authors read and approved the final version of the manuscript.

Notes

The authors declare no competing financial interest.

■ ACKNOWLEDGMENTS

This research was funded by Sub-project of Innovation Team and Talents cultivation Program of National Administration of Traditional Chinese Medicine (No. ZYYCXTD-C-202005-11), National Special Support Plan Project for High-level Talents (Plan of Ten Thousand Talents) Famous Teacher, the National Natural Science Foundation of China (No. 81874349), and the Key Project for Basic Research Fund of Beijing University of Chinese Medicine (No. 2020-JYB-20GG-047). The authors would like to thank Prof. Jian Ni for the gift of HepG2 cell lines.

■ ABBREVIATIONS

CH:citrus herb; CYP450:cytochrome P450; ECG:Exocarpium Citri Grandis; ECR:Exocarpium Citri Rubrum; FA:Fructus Aurantii; FAI:Fructus Aurantii Immaturus; FC:Fructus Citri; FCS:Fructus Citri Sarcodactylis; GF:grapefruit; GO:gene ontology; HDI:herb–drug interaction; KEGG:Kyoto Encyclopedia of Genes and Genomes; OATP:organic anion transporting polypeptide; PCR:Pericarpium Citri Reticulatae; PCRV:Pericarpium Citri Reticulatae Viride; P-gp:P-glycoprotein; PPI:protein–protein interaction; TCMSP:Traditional Chinese Medicine Systems Pharmacology Database and Analysis Platform

■ REFERENCES

(1) Singh, A.; Zhao, K. Herb-Drug Interactions of Commonly Used Chinese Medicinal Herbs. *Int. Rev. Neurobiol.* **2017**, *135*, 197–232.

(2) Hyson, D. A. A review and critical analysis of the scientific literature related to 100% fruit juice and human health. *Adv. Nutr.* **2015**, *6*, 37−51.
(3) Seden, K.; Dickinson, L.; Khoo, S.; Back, D. Grapefruit-drug interactions. *Drugs* **2010**, *70*, 2373−2407.
(4) Chen, S.; Peng, Y.; Chen, S.; Xiao, P. Introduction of Pharmaphylogeny. *Mod. Tradit. Chin. Med. Mater. Med.-World Sci. Technol.* **2005**, *7*, 97−103.
(5) Dugrand-Judek, A.; Olry, A.; Hehn, A.; Costantino, G.; Ollitrault, P.; Froelicher, Y.; Bourgaud, F. The Distribution of Coumarins and Furanocoumarins in Citrus Species Closely Matches Citrus Phylogeny and Reflects the Organization of Biosynthetic Pathways. *PLoS One* **2015**, *10*, No. e0142757.
(6) Yu, X.; Sun, S.; Guo, Y.; Liu, Y.; Yang, D.; Li, G.; Lu, S. Citri Reticulatae Pericarpium (Chenpi): Botany, ethnopharmacology, phytochemistry, and pharmacology of a frequently used traditional Chinese medicine. *J. Ethnopharmacol.* **2018**, *220*, 265−282.
(7) Egashira, K.; Fukuda, E.; Onga, T.; Yogi, Y.; Matsuya, F.; Koyabu, N.; Ohtani, H.; Sawada, Y. Pomelo-induced increase in the blood level of tacrolimus in a renal transplant patient. *Transplantation* **2003**, *75*, No. 1057.
(8) Hopkins, A. L. Network pharmacology. *Nat. Biotechnol.* **2007**, *25*, 1110−1111.
(9) Kiani, J.; Imam, S. Z. Medicinal importance of grapefruit juice and its interaction with various drugs. *Nutr. J.* **2007**, *6*, No. 33.
(10) Lin, S. P.; Chao, P. D.; Tsai, S. Y.; Wang, M. J.; Hou, Y. C. Citrus grandis peel increases the bioavailability of cyclosporine and tacrolimus, two important immunosuppressants, in rats. *J. Med. Food* **2011**, *14*, 1463−1468.
(11) Lin, S. P.; Wu, P. P.; Hou, Y. C.; Tsai, S. Y.; Wang, M. J.; Fang, S. H.; Chao, P. D. Different influences on tacrolimus pharmacokinetics by coadministrations of zhi ke and zhi shi in rats. *Evidence-Based Complementary Altern. Med.* **2011**, *2011*, No. 751671.
(12) Ahmed, I. S.; Hassan, M. A.; Kondo, T. Effect of lyophilized grapefruit juice on P-glycoprotein-mediated drug transport in-vitro and in-vivo. *Drug Dev. Ind. Pharm.* **2015**, *41*, 375−381.
(13) Lin, H. L.; Kenaan, C.; Hollenberg, P. F. Identification of the residue in human CYP3A4 that is covalently modified by bergamottin and the reactive intermediate that contributes to the grapefruit juice effect. *Drug Metab. Dispos.* **2012**, *40*, 998−1006.
(14) Rebello, S.; Zhao, S.; Hariry, S.; Dahlke, M.; Alexander, N.; Vapurcuyan, A.; Hanna, I.; Jarugula, V. Intestinal OATP1A2 inhibition as a potential mechanism for the effect of grapefruit juice on aliskiren pharmacokinetics in healthy subjects. *Eur. J. Clin. Pharmacol.* **2012**, *68*, 697−708.
(15) Liu, D.; Wu, J.; Xie, H.; Liu, M.; Takau, I.; Zhang, H.; Xiong, Y.; Xia, C. Inhibitory Effect of Hesperetin and Naringenin on Human UDP-Glucuronosyltransferase Enzymes: Implications for Herb-Drug Interactions. *Biol. Pharm. Bull.* **2016**, *39*, 2052−2059.
(16) Kondža, M.; Bojic, M.; Tomic, I.; Males, Z.; Rezic, V.; Cavar, I. Characterization of the CYP3A4 Enzyme Inhibition Potential of Selected Flavonoids. *Molecules* **2021**, *26*, No. 3018.
(17) Weiss, J.; Gattuso, G.; Barreca, D.; Haefeli, W. E. Nobiletin, sinensetin, and tangeretin are the main perpetrators in clementines provoking food-drug interactions in vitro. *Food Chem.* **2020**, *319*, No. 126578.
(18) Šarić Mustapić, D.; Debeljak, Z.; Males, Z.; Bojic, M. The Inhibitory Effect of Flavonoid Aglycones on the Metabolic Activity of CYP3A4 Enzyme. *Molecules* **2018**, *23*, No. 2553.
(19) Walsky, R. L.; Bauman, J. N.; Bourcier, K.; Giddens, G.; Lapham, K.; Negahban, A.; Ryder, T. F.; Obach, R. S.; Hyland, R.; Goosen, T. C. Optimized assays for human UDP-glucuronosyltransferase (UGT) activities: altered alamethicin concentration and utility to screen for UGT inhibitors. *Drug Metab. Dispos.* **2012**, *40*, 1051−1065.
(20) Tornio, A.; Backman, J. T. Cytochrome P450 in Pharmacogenetics: An Update. *Adv. Pharmacol.* **2018**, *83*, 3−32.
(21) Veronese, M. L.; Gillen, L. P.; Burke, J. P.; Dorval, E. P.; Hauck, W. W.; Pequignot, E.; Waldman, S. A.; Greenberg, H. E. Exposure-dependent inhibition of intestinal and hepatic CYP3A4 in vivo by grapefruit juice. *J. Clin. Pharmacol.* **2003**, *43*, 831−839.
(22) Greenblatt, D. J.; von Moltke, L. L.; Harmatz, J. S.; Chen, G.; Weemhoff, J. L.; Jen, C.; Kelley, C. J.; LeDuc, B. W.; Zinny, M. A. Time course of recovery of cytochrome p450 3A function after single doses of grapefruit juice. *Clin. Pharmacol. Ther.* **2003**, *74*, 121−129.
(23) Hollander, A. A. M. J.; van Rooij, J.; Lentjes, G. W.; Arbouw, F.; van Bree, J. B.; Schoemaker, R. C.; van Es, L. A.; van der Woude, F. J.; Cohen, A. F. The effect of grapefruit juice on cyclosporine and prednisone metabolism in transplant patients. *Clin. Pharmacol. Ther.* **1995**, *57*, 318−324.
(24) Zhou, L.; Cui, M.; Zhao, L.; Wang, D.; Tang, T.; Wang, W.; Wang, S.; Huang, H.; Qiu, X. Potential Metabolic Drug-Drug Interaction of Citrus aurantium L. (Rutaceae) Evaluating by Its Effect on 3 CYP450. *Front. Pharmacol.* **2018**, *9*, No. 895.
(25) Guo, L. Q.; Taniguchi, M.; Chen, Q. Y.; Baba, K.; Yamazoe, Y. Inhibitory potential of herbal medicines on human cytochrome P450-mediated oxidation: properties of umbelliferous or citrus crude drugs and their relative prescriptions. *Jpn. J. Pharmacol.* **2001**, *85*, 399−408.
(26) Rowland, A.; Miners, J. O.; Mackenzie, P. I. The UDP-glucuronosyltransferases: their role in drug metabolism and detoxification. *Int. J. Biochem. Cell Biol.* **2013**, *45*, 1121−1132.
(27) Saracino, M. R.; Bigler, J.; Schwarz, Y.; Chang, J. L.; Li, S.; Li, L.; White, E.; Potter, J. D.; Lampe, J. W. Citrus fruit intake is associated with lower serum bilirubin concentration among women with the UGT1A1*28 polymorphism. *J. Nutr.* **2009**, *139*, 555−560.
(28) Liu, X. Transporter-Mediated Drug-Drug Interactions and Their Significance. *Adv. Exp. Med. Biol.* **2019**, *1141*, 241−291.
(29) Panchagnula, R.; Bansal, T.; Varma, M. V.; Kaul, C. L. Co-treatment with grapefruit juice inhibits while chronic administration activates intestinal P-glycoprotein-mediated drug efflux. *Pharmazie* **2005**, *60*, 922−927.
(30) Okada, N.; Murakami, A.; Urushizaki, S.; Matsuda, M.; Kawazoe, K.; Ishizawa, K. Extracts of Immature Orange (Aurantii fructus immaturus) and Citrus Unshiu Peel (Citri unshiu pericarpium) Induce P-Glycoprotein and Cytochrome P450 3A4 Expression via Upregulation of Pregnane X Receptor. *Front. Pharmacol.* **2017**, *8*, No. 84.
(31) Bailey, D. G.; Dresser, G. K.; Leake, B. F.; Kim, R. B. Naringin is a major and selective clinical inhibitor of organic anion-transporting polypeptide 1A2 (OATP1A2) in grapefruit juice. *Clin. Pharmacol. Ther.* **2007**, *81*, 495−502.
(32) Shirasaka, Y.; Mori, T.; Murata, Y.; Nakanishi, T.; Tamai, I. Substrate- and dose-dependent drug interactions with grapefruit juice caused by multiple binding sites on OATP2B1. *Pharm. Res.* **2014**, *31*, 2035−2043.
(33) Strauch, K.; Lutz, U.; Bittner, N.; Lutz, W. K. Dose-response relationship for the pharmacokinetic interaction of grapefruit juice with dextromethorphan investigated by human urinary metabolite profiles. *Food Chem. Toxicol.* **2009**, *47*, 1928−1935.
(34) Fukuda, K.; Ohta, T.; Oshima, Y.; Ohashi, N.; Yoshikawa, M.; Yamazoe, Y. Specific CYP3A4 inhibitors in grapefruit juice: furocoumarin dimers as components of drug interaction. *Pharmacogenetics* **1997**, *7*, 391−396.
(35) Mohri, K.; Uesawa, Y. Effects of furanocoumarin derivatives in grapefruit juice on nifedipine pharmacokinetics in rats. *Pharm. Res.* **2001**, *18*, 177−182.
(36) Paine, M. F.; Criss, A. B.; Watkins, P. B. Two major grapefruit juice components differ in intestinal CYP3A4 inhibition kinetic and binding properties. *Drug Metab. Dispos.* **2004**, *32*, 1146−1153.
(37) Fuhr, U.; Klittich, K.; Staib, A. H. Inhibitory effect of grapefruit juice and its bitter principal, naringenin, on CYP1A2 dependent metabolism of caffeine in man. *Br. J. Clin. Pharmacol.* **1993**, *35*, 431−436.
(38) Han, Y. L.; Yu, H. L.; Li, D.; Meng, X. L.; Zhou, Z. Y.; Yu, Q.; Zhang, X. Y.; Wang, F. J.; Guo, C. Inhibitory effects of limonin on six human cytochrome P450 enzymes and P-glycoprotein in vitro. *Toxicol. In Vitro* **2011**, *25*, 1828−1833.

https://doi.org/10.1021/acsomega.2c04579
ACS Omega 2022, 7, 35911−35923

(39) Ma, W.; Feng, S.; Yao, X.; Yuan, Z.; Liu, L.; Xie, Y. Nobiletin enhances the efficacy of chemotherapeutic agents in ABCB1 overexpression cancer cells. *Sci. Rep.* **2015**, *5*, No. 18789.
(40) Shanghai Institute of Organic Chemistry, Chinese Academy of Sciences. Chemistry Database, 1978−2020. http://www.organchem.csdb.cn.
(41) Ru, J.; Li, P.; Wang, J.; Zhou, W.; Li, B.; Huang, C.; Li, P.; Guo, Z.; Tao, W.; Yang, Y.; et al. TCMSP: a database of systems pharmacology for drug discovery from herbal medicines. *J. Cheminf.* **2014**, *6*, No. 13.
(42) Kim, S.; Thiessen, P. A.; Bolton, E. E.; Chen, J.; Fu, G.; Gindulyte, A.; Han, L.; He, J.; He, S.; Shoemaker, B. A.; et al. PubChem Substance and Compound databases. *Nucleic Acids Res.* **2016**, *44*, D1202−1213.
(43) Daina, A.; Michielin, O.; Zoete, V. SwissADME: a free web tool to evaluate pharmacokinetics, drug-likeness and medicinal chemistry friendliness of small molecules. *Sci. Rep.* **2017**, *7*, No. 42717.
(44) Lipinski, C. A.; Lombardo, F.; Dominy, B. W.; Feeney, P. J. Experimental and computational approaches to estimate solubility and permeability in drug discovery and development settings. *Adv Drug Delivery Rev.* **2001**, *46*, 3−26.
(45) Daina, A.; Michielin, O.; Zoete, V. SwissTargetPrediction: updated data and new features for efficient prediction of protein targets of small molecules. *Nucleic Acids Res.* **2019**, *47*, W357−W364.
(46) Szklarczyk, D.; Santos, A.; von Mering, C.; Jensen, L. J.; Bork, P.; Kuhn, M. STITCH 5: augmenting protein-chemical interaction networks with tissue and affinity data. *Nucleic Acids Res.* **2016**, *44*, D380−384.
(47) Oliveros, J. C. Venny. An Interactive Tool for Comparing Lists with Venn's Diagrams, 2007−2015. https://bioinfogp.cnb.csic.es/tools/venny/index.html.
(48) Shannon, P.; Markiel, A.; Ozier, O.; Baliga, N. S.; Wang, J. T.; Ramage, D.; Amin, N.; Schwikowski, B.; Ideker, T. Cytoscape: a software environment for integrated models of biomolecular interaction networks. *Genome Res.* **2003**, *13*, 2498−2504.
(49) Krzywinski, M.; Schein, J.; Birol, I.; Connors, J.; Gascoyne, R.; Horsman, D.; Jones, S. J.; Marra, M. A. Circos: an information aesthetic for comparative genomics. *Genome Res.* **2009**, *19*, 1639−1645.
(50) Szklarczyk, D.; Gable, A. L.; Lyon, D.; Junge, A.; Wyder, S.; Huerta-Cepas, J.; Simonovic, M.; Doncheva, N. T.; Morris, J. H.; Bork, P.; et al. STRING v11: protein-protein association networks with increased coverage, supporting functional discovery in genome-wide experimental datasets. *Nucleic Acids Res.* **2019**, *47*, D607−D613.
(51) Wishart, D. S.; Feunang, Y. D.; Guo, A. C.; Lo, E. J.; Marcu, A.; Grant, J. R.; Sajed, T.; Johnson, D.; Li, C.; Sayeeda, Z.; et al. DrugBank 5.0: a major update to the DrugBank database for 2018. *Nucleic Acids Res.* **2018**, *46*, D1074−D1082.
(52) Whirl-Carrillo, M.; McDonagh, E. M.; Hebert, J. M.; Gong, L.; Sangkuhl, K.; Thorn, C. F.; Altman, R. B.; Klein, T. E. Pharmacogenomics knowledge for personalized medicine. *Clin. Pharmacol. Ther.* **2012**, *92*, 414−417.
(53) Huang, D. W.; Sherman, B. T.; Lempicki, R. A. Systematic and integrative analysis of large gene lists using DAVID bioinformatics resources. *Nat. Protoc.* **2009**, *4*, 44−57.
(54) Huang, D. W.; Sherman, B. T.; Lempicki, R. A. Bioinformatics enrichment tools: paths toward the comprehensive functional analysis of large gene lists. *Nucleic Acids Res.* **2009**, *37*, 1−13.
(55) Jumper, J.; Evans, R.; Pritzel, A.; Green, T.; Figurnov, M.; Ronneberger, O.; Tunyasuvunakool, K.; Bates, R.; Zidek, A.; Potapenko, A.; et al. Highly accurate protein structure prediction with AlphaFold. *Nature* **2021**, *596*, 583−589.
(56) Varadi, M.; Anyango, S.; Deshpande, M.; Nair, S.; Natassia, C.; Yordanova, G.; Yuan, D.; Stroe, O.; Wood, G.; Laydon, A.; et al. AlphaFold Protein Structure Database: massively expanding the structural coverage of protein-sequence space with high-accuracy models. *Nucleic Acids Res.* **2022**, *50*, D439−D444.
(57) Adasme, M. F.; Linnemann, K. L.; Bolz, S. N.; Kaiser, F.; Salentin, S.; Haupt, V. J.; Schroeder, M. PLIP 2021: expanding the scope of the protein-ligand interaction profiler to DNA and RNA. *Nucleic Acids Res.* **2021**, *49*, W530−W534.

https://doi.org/10.1021/acsomega.2c04579
ACS Omega 2022, 7, 35911−35923